THE SCIENCE AND CULTURE SERIES — PHYSICS

Proceedings of the 20th Workshop of the INFN Eloisatron Project

GaAs Detectors and Electronics for High-Energy Physics

Erice, Trapani, Italy 12 – 18 January 1992

Editors
C. del Papa
P. G. Pelfer
K. Smith

Series Editor
A. Zichichi

World Scientific
Singapore • New Jersey • London • Hong Kong

Published by

World Scientific Publishing Co. Pte. Ltd.
P O Box 128, Farrer Road, Singapore 9128
USA office: Suite 1B, 1060 Main Street, River Edge, NJ 07661
UK office: 73 Lynton Mead, Totteridge, London N20 8DH

GaAs Detectors and Electronics for High-Energy Physics

ISBN 981-02-1148-1

Printed in Singapore by JBW Printers & Binders Pte. Ltd.

CONTENTS

FABRICATION AND EVALUATION OF ROOM TEMPERATURE OPERATED RADIATION DETECTORS PROCESSED FROM UNDOPED LEC BULK GALLIUM ARSENIDE MATERIAL

D.S. McGREGOR and G.F. KNOLL
Department of Nuclear Engineering, University of Michigan, Cooley Building
Ann Arbor, Michigan 48109-2104, U.S.A.

Y. EISEN
Soreq Nuclear Research Center, Israel Atomic Energy Commission
Yavne 70600, Israel

and

R. BRAKE
Radiation Protection Group, Los Alamos National Laboratory
Los Alamos, New Mexico 87545, U.S.A

ABSTRACT

Semi-insulating undoped bulk LEC GaAs was investigated as a possible detector material for room temperature operated charged particle and gamma ray spectrometers. GaAs Schottky based diode detectors were fabricated with thicknesses of 45 microns, 100 microns, 250 microns, and 750 microns. Pulse height analysis utilizing an alpha particle source disclosed non-constant electric field distributions that decreased rapidly from the Schottky contact into the bulk of the detectors. Results from pulsed X-ray analysis and the alpha particle pulse height analysis indicate an active region width voltage dependence that strongly deviates from $\sqrt{V}$ behavior. Resolution at room temperature for ^{241}Am alpha particles ranged from 2.2% to 3.1% FWHM for different detectors with a typical resolution of 2.5% FWHM. Room temperature measurements of 60 keV gamma rays (^{241}Am) and 122 keV gamma rays (^{57}Co) resulted in observed full energy peaks with FWHM's of 22 keV and 40 keV, respectively.

1. Introduction

GaAs has material characteristics that suggest that it may be used as a room temperature operated radiation spectrometer[1,2]. Previous results tend to confirm its possible use for high resolution charged particle and gamma ray spectroscopy[3,4]. Unfortunately, high resolution detectors have generally been restricted to very thin epitaxial crystals grown by either LPE or VPE methods. These epitaxial detectors are normally 100 microns or less in thickness, which translates to very inefficient interaction probabilities for gamma rays of energies above 150 keV. In order to produce gamma ray detectors useful at higher energies, it will be necessary to fabricate detectors of greater thickness. Due to expense and technological difficulties, it is not practical to produce epitaxial GaAs detectors approaching 1 mm in thickness. However, high quality bulk grown liquid encapsulated Czochralski (LEC) GaAs single crystal material offers an attractive low cost alternative to epitaxial crystals.

An understanding of bulk GaAs material electrical characteristics is necessary if it is to be seriously considered as a viable room temperature semiconductor detector candidate. Early work on bulk LEC GaAs detectors revealed unexpected behavior from the material[5]. For instance, calculated depletion depths utilizing measured carrier concentrations were quite different from observed results and capacitance-voltage (C-V) measurements yielded no information as to the depletion characteristics. The following article is devoted to describing the method by which our detectors were fabricated and tested with some suggestions as to the reasons for their behavior.

2. Detector Fabrication

Undoped LEC GaAs wafers were diced into 5.08 x 5.08 mm squares and attached to quartz polishing flats with Crystalbond 509. The pieces were polished using a solution of 1:15:30 Bromine:Glycerol:Methanol in conjunction with polishing pads (Buehler TEXMET No. 40-7618 for rough polishing and Buehler Chemomet No. 40-7918 for fine polishing). Bromine based solutions can corrode several different types of metallic flats, therefore the polishing pads were attached to quartz optical flats. The GaAs pieces were polished to final thicknesses of 45 microns, 100 microns, 250 microns, and 750 microns.

Metals can contaminate GaAs and destroy the soft crystal, therefore the pieces were handled in such a way that metal objects no longer came into contact with the GaAs surfaces. Thick pieces were handled with teflon tweezers and thin pieces (less than 50 microns) were handled with teflon vacuum tools. The pieces were cleaned in a class 100 clean room in the order as follows:

Ultrasonically cleaned 5 minutes in TCE
Ultrasonically cleaned 5 minutes in acetone
Ultrasonically cleaned 5 minutes in isopropal alcohol (IPA)
Ultrasonically cleaned 5 minutes in methyl alcohol (METH)
Ultrasonically cleaned 5 minutes in deionized water (DI)
Ultrasonically cleaned 5 minutes in 1:1:320 H_2SO_4:H_2O_2:DI
Washed and ultrasonically cleaned 5 minutes in DI
Washed 2 minutes in 1:1 HCl:DI
Washed and ultrasonically cleaned 5 minutes in DI
Blown dry with nitrogen
Baked at 90°C in nitrogen atmosphere for 5 minutes

5000 Å of Si_3N_4 were plasma deposited onto the ohmic contact sides to provide passivation and protection during processing. Photoresist was patterned to protect 4.32 mm diameter circular regions on the Schottky contact sides of the pieces. Afterwards, the Schottky contact sides were implanted with 60 keV protons at a dose of $10^{16}/cm^2$ in order to create traps and reduce surface leakage current. Implantation

was performed with the crystals oriented 7° off the flat to prevent channeling. The photoresist was removed and the pieces were cleaned again as previously described without the H_2SO_4 step. A 5000 Å layer of Si_3N_4 was then plasma deposited on the Schottky contact sides.

Photoresist was spun onto the ohmic contact sides and 4.32 mm diameter circular regions were patterned in the center of the pieces. The backsides were protected with photoresist as well. The Si_3N_4 layers were wet etched to the bare GaAs surfaces. After a DI rinse, the pieces were placed in a shadow mask with 4.6 mm diameter circular openings to prevent metal evaporation on the edges. The shadow mask was placed into an e-beam evaporator and a series of Au, Ge, and Ni layers were evaporated onto the pieces in the order as follows:

50 Å - Ni
110 Å - Ge
225 Å - Au
50 Å - Ni
220 Å -Ge
450 Å - Au
50 Å - Ni
400 Å - Au

The metal layers overlapping the photoresist were lifted off with acetone, followed by a rinse in IPA, METH, and DI. The contacts were rapid thermally annealed in a nitrogen atmosphere at 410°C for 1 minute.

The Schottky contact sides were then patterned as previously described and the Si_3N_4 was etched to the bare GaAs. The photoresist was removed and the pieces were cleaned as previously described excluding the step with H_2SO_4:H_2O_2:DI (since it attacks the Au/Ge/Ni contacts). Each GaAs piece was bonded into a boron nitride (BN) collar with high resistivity potting epoxy (Ciba Geigy 1:2 HY837 hardener:GY502 resin). Afterwards, brass connector rings designed to accept either BNC or SHV connectors were epoxied to the BN collars. After the epoxy cured (at room temperature), the packaged pieces were cleaned in acetone, IPA, METH, and DI, followed by a N_2 blow dry. With an eyedropper, a solution of H_2SO_4:H_2O_2:DI was carefully placed onto the bare GaAs on the Schottky contact sides of the devices and allowed to sit for 2 minutes. The packages were then thoroughly rinsed in DI water. Using an eyedropper again, a solution of 1:1 HCl:DI was placed onto the bare GaAs surfaces for a duration of two minutes followed by a thorough DI rinse. The packages were carefully dried with N_2.

All of the packages were placed into an e-beam evaporator with the Schottky contact side exposed to the pocket. A 150 Å layer of Ti followed by a 350 Å layer of Au was evaporated over the surfaces to form a Schottky contact. The packages were then turned over and a 150 Å layer of Ti followed by a 350 Å layer of Au was evaporated over the ohmic contacts in order to make electrical contact to the brass connector rings. Electrical connectors were then fastened to the detectors. A cross section diagram of a finished detector can be seen in figure 1.

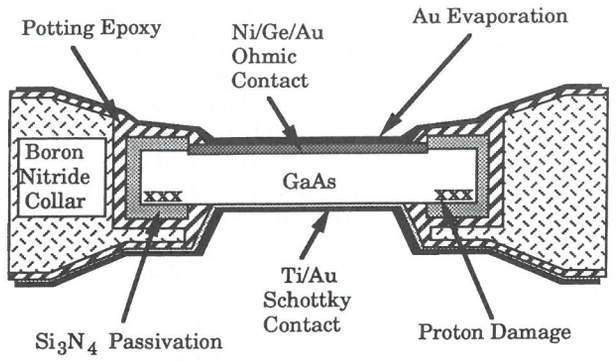

Figure 1. Cross section diagram of a Schottky barrier GaAs detector.

3. Theoretical Considerations

The basic device investigated consisted of one Schottky contact and one alloyed ohmic contact. Such a configuration creates a Schottky barrier diode in which rectifying behavior is observed under voltage bias. The current density behavior of a Schottky diode can generally be described by

$$J(V) = J_{st}(e^{Vq/nkT} - 1) \tag{1}$$

where

$$J_{st} = A^*T^2e^{-V_Bq/kT} \tag{2}$$

and V is the applied voltage, n is the ideality factor, V_B is the Schottky barrier potential, and A^* is the effective Richardson constant[6]. Under reverse bias, the current density is very low and increases only slightly until a breakdown voltage is exceeded. Diode detectors are commonly operated under reverse bias in which free carriers are removed leaving a space charge region. The electric field present across the detector space charge region allows for the extraction of electrons and holes excited from ionizing radiation interactions in the material. The current induced by the motion of electrons and holes in the detector charges an equivelent capacitance that allows for a relative measurement of energy deposition.

Two theoretical models demonstrating extreme conditions are the intrinsic device with some possible trapping and the extrinsic device characterized by the carrier concentration present from shallow ionized impurities. In the intrinsic case, we assume that the free carrier concentration present is due primarily to thermal ionization of states in the valence band with a small additional component from background dopants. The intrinsic carrier concentration as a function of temperature can be described by[7]

$$p_o(T) = n_o(T) = n_i(T) = 2\left(\frac{2\pi(m_h^*m_e^*)^{1/2}kT}{\hbar^2}\right)^{3/2}e^{-(E_c-E_v)/2kT} \tag{3}$$

where m^* is the carrier effective mass. The background donor concentration is defined as ν and the background acceptor concentration is defined as π. The values of n_o and p_o are perturbed from their intrinsic values in the presence of background dopants. If it is assumed that only a light background doping component is present, then the charge present in the depletion region is simply the net ionized concentration of light dopants and the concentration of thermally generated carriers. Assuming that the thermally generated free carriers are removed quickly so that a space charge region is defined by the stationary ionized background dopants, from Poisson's equation

$$-\frac{\partial^2 V}{\partial x^2} = \frac{\partial \mathcal{E}}{\partial x} = \frac{\rho}{\epsilon_s} = \frac{q(\nu^+ - \pi^-)}{\epsilon_s} \tag{4}$$

it is found that the space charge region width as a function of voltage for a Schottky diode is described by the one-sided abrupt junction approximation

$$W(V) = \sqrt{\frac{2\epsilon_s(V_B - V)}{q|(\nu^+ - \pi^-)|}} \tag{5}$$

and the electric field as a function of width is

$$\mathcal{E}(x) = -\frac{q(\nu^+ - \pi^-)}{\epsilon_s}(W - x) \quad . \tag{6}$$

If the material is perfectly compensated so that the stationary charge from the background dopants cancel (or $\nu^+ = \pi^-$), then equation 4 can be solved to show that the electric field is constant and the active width of the detector is simply the detector width. For a thin detector, the assumption can be made that the electric field is simply the voltage divided by the detector width and the active detector region extends completely across the device.

If a packet of charge were to be created at a point location in the device, the total charge induced on the charging capacitor would be represented by

$$Q = \frac{N_o q}{W}\left[\frac{\tau_e x_e}{t_e}(1 - e^{-t_e/\tau_e}) + \frac{\tau_h x_h}{t_h}(1 - e^{-t_h/\tau_h})\right] \tag{7}$$

where N_o is the total number of charge carriers created in the detector during the ionizing incident, W is the total detector active region width, x denotes the distance that a particular carrier must travel to be removed from the device, t is the required time for a carrier to travel distance x, τ is the carrier lifetime, and the e and h subscripts denote electrons and holes, respectively. With zero applied voltage, only the barrier potential V_B appears across the active region, and the small electric field results in slow charge drift with considerable loss to recombination. As the field strength is increased, the carrier velocities increase and charge recombination is reduced. At high electric field strengths, the carriers reach a saturated velocity and the expected result is a maximum achievable pulse height. In the presence of trapping, the pulse height is reduced from the case of no trapping.

The location at which charge is created is randomly distributed through the detector for high energy gamma rays, and skewed towards the exposed detector face

for alpha particles and low energy X-rays. For the example of alpha particles, specific ionization in a material is described by the Bragg distribution[8]

$$I(d) = \int_d^\infty \frac{i(r-d)}{\alpha\sqrt{\pi}} e^{-[(r-R)/\alpha]^2} dr \tag{8}$$

where r is the range of an individual particle, R is the mean range of the particles, d is the distance that the particle has penetrated into the detector, α is the straggling parameter, and the term $i(r-d)$ defines the specific ionization along the path of an individual particle at the distance $(r-d)$ from the end of its path. The Bragg distribution shows that the greatest density of ionization occurs near the end of the particle range. As charged particles enter from the detector front (assuming the detector thickness is more than twice the alpha particle range), a larger portion of the induced charge will be from the electrons since, in the absence of trapping, they travel further in the detector. However, if irradiated from the back, the larger contribution of induced charge will be from the holes. If the holes undergo severe trapping and the electrons do not, we would expect the limiting pulse height at carrier saturation velocity from front side irradiation to be greater than observed from back side irradiation.

As a simple model of the expected pulse height from an 100 micron intrinsic GaAs detector, we assume that all of the charge is created in a plane at the end of a 5.5 MeV alpha particle range. The range of a 5.5 MeV alpha particle is approximately 20 microns in GaAs. Therefore, if all of the charge is collected from front side irradiation (no trapping), 80% of the pulse height will be due to electron movement and 20% of the pulse height will be due to hole movement. If irradiated from the back, the opposite case will be true in which 20% of the pulse height is due to electron movement and 80% of the pulse height is due to hole movement. If the electrons and holes undergo trapping, the pulse height becomes a function of the total charge collected as described in equation 7. Since electrons and holes have different velocity characteristics, the number of electrons and holes trapped will differ per unit time although they may have the same lifetime. Figure 2 shows theoretical normalized pulse height curves for a 100 micron intrinsic GaAs detector with equal carrier lifetimes of 5 nanoseconds and 0.5 nanoseconds. The figure indicates that we would expect to see pulses at low bias voltages whether the detector were irradiated from the front or the back since electrons and holes will contribute to some amount of induced current even at low voltages and short carrier lifetimes.

In the case of an extrinsic detector with only shallow dopants that are fully ionized and evenly distributed, Poisson's equation becomes

$$-\frac{\partial^2 V}{\partial x^2} = \frac{\partial \mathcal{E}}{\partial x} = \frac{\rho}{\epsilon_s} = \frac{q}{\epsilon_s}(N_d^+ - N_a^- - n_o) \tag{9}$$

where N_d^+ is the ionized donor concentration and N_a^- is the ionized acceptor concentration. The solution is similar as before, except $(\nu^+ - \pi^-)$ is replaced by the concentration of net ionized dopant atoms, hence

$$W(V) = \sqrt{\frac{2\epsilon_s(V_B - V)}{q|N_b|}} \tag{10}$$

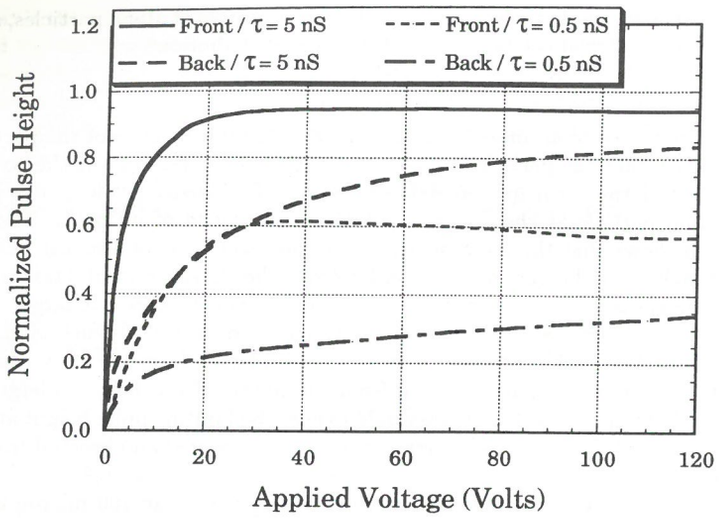

Figure 2. Theoretical normalized voltage dependent pulse height curves for a fully depleted 100 micron intrinsic GaAs diode detector. Shown are predicted curves for front and back irradiation from alpha particles that hypothetically deposit their total energy at a depth of 20 microns. Also shown are results for both charge carriers having lifetimes of 5 nanoseconds and both charge carriers having lifetimes of 0.5 nanoseconds.

where

$$N_b = N_d^+ - N_a^- \quad , \tag{11}$$

and the electric field as a function of width is

$$\mathcal{E}(x) = -\frac{qN_b}{\epsilon_s}(W - x) \quad . \tag{12}$$

If the value of N_b is very small, the results are similar to the intrinsic or perfectly compensated detector in which the electric field is constant and the space charge region extends across the width of the detector. However, if N_b is large, it is no longer valid to assume that the electric field is constant, and the space charge region extends a finite distance into the detector. At low electric field values, the efficiency of carrier extraction decreases due to low carrier velocities, therefore, we refer to the volume of the space charge region that allows for carrier extraction as the detector active region.

In a Schottky diode detector with no trapping, the pulse height will be determined by the amount of energy deposited within the active region. Thus, the pulse height observed is a function of the active region width coupled with the energy deposition characteristics of the particle. Referring to figure 3a, as the active region extends from point A to point B, the pulse height is expected to increase slowly because the energy deposition from the alpha particle is slowly varying. With higher bias voltage, the active region increases from point B to point C and more of the energy deposited by the particle contributes to the pulse height. Also, since the energy deposition per distance is increasing, the pulse height increases nonlinearly with applied bias. As the active region is increased beyond point D, the pulse height no longer increases since all of the energy from the alpha particle is fully deposited in the active region. Now referring to figure 3b, if the same detector were to be irradiated from the back, no pulses would be observed until the applied voltage increased the active region to point C. Since a large fraction of the alpha particle energy is deposited near the end of its path, the expected result is a large increase in pulse height as the active region extends beyond point C. The pulse height no longer increases when the detector becomes fully depleted (point F). Thus in the extrinsic case, it is expected that pulses will be observed from front side irradiation at low bias voltages, and a threshold voltage exists at which pulses will be observed under back side irradiation. If trapping were to become an issue, there would be a decrease in the observed saturated pulse height, however, the pulse height curves would retain their characteristic shape.

4. Detector Results and Analysis

I-V measurements indicated that the detectors were severely space charge limited. Under forward bias, the current density ideality factor ranged from 5 to over 40 and the turn-on voltage increased non-linearly with detector thickness[5]. The reverse current density was not dependent on the detector thickness. Modulated *C-V* measurements indicated no change in capacitance with increasing reverse voltage for all detectors tested[5]. Although such behavior observed from a modulated *C-V* measurement is often interpreted as full depletion of a detector, the deep level traps and the high resistivity of semi-insulating GaAs can lead to erroneous results [9,10]. If the detectors behaved as intrinsic or high purity devices (as suggested by the *C-V* measurements), the expected electric field distribution would be fairly constant with a gradually decreasing slope described by equation 6.

Monte-Carlo analysis of 5.5 MeV alpha particles indicates that their range in GaAs is 20.2 microns with a straggling of 0.45 microns[11]. Since 20 microns is approximately half the thickness of the 45 micron detectors, a significant number of electrons and holes would be created near the center of the detectors whether they are irradiated from the front or back. If the intrinsic model describes the detector active region, then pulses should be seen at very low bias voltages from front side irradiation and back side irradiation even if one type of carrier is severely trapped. However, if the extrinsic model describes the detector active region, pulses will be observed from front side irradiation at low bias voltages and pulses will not be observed from back side irradiation until a threshold voltage is reached.

Figures 4 and 5 show the results from two detectors with 43 and 105 micron

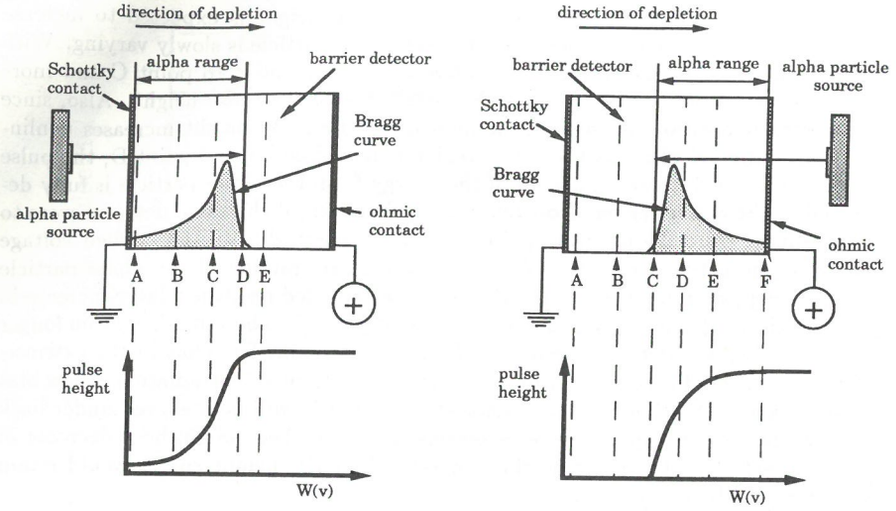

Figure 3. Expected voltage dependent pulse height curve shapes from an extrinsic GaAs diode detector. Figure 3a depicts the expected pulse height response due to front side irradiation and figure 3b depicts the expected pulse height response due to back side irradiation from monoenergetic alpha particles. Pulses are observed at low voltages when irradiated from the front, however, pulses are not observed from back side irradition until a threshold voltage is reached.

thicknesses irradiated with alpha particles separately from the front and back. The 43 micron detector revealed observed pulses at low bias voltages when irradiated from the front, reaching a saturated value at approximately 55 volts. However, pulses were not observed from back side irradiation until a threshold voltage of approximately 55 volts was reached. The alpha particle average energy and range were decreased with thin aluminum attenuators and the observed plateau voltage for front side irradiation decreased as expected. With the attenuators in place, the threshold voltage from back side irradiation was observed to increase with increasing attenuator mass (figure 4). The 105 micron detector (figure 5) also revealed observed pulses at low bias voltages when irradiated from the front, and the pulse height saturated at a value near 60 volts. The threshold voltage from back side irradiation increased to 105 volts.

Of interest is the fact that the pulse height curves from front side irradiation for the 43 micron detector and the 105 micron detector are very similar although one is 2.4 times thicker than the other. Such behavior suggests that the electric field distribution near the Schottky contact is similar for both detectors. Therefore, we conclude that the extrinsic model is valid and the intrinsic model is not, and the detectors are not fully depleted in the conventional sense. However, if the threshold

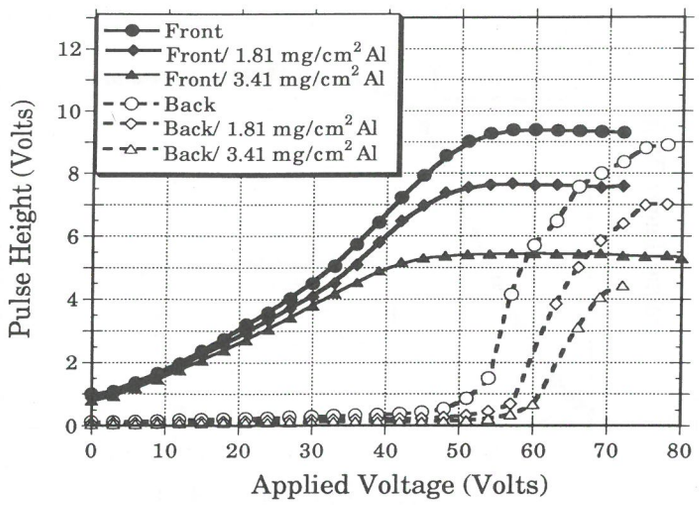

Figure 4. Measured voltage dependent pulse height response from a 43 micron GaAs Schottky diode detector. Shown are curves corresponding to front and back irradiation of the detector with 5.5 MeV ^{241}Am alpha particles in a vacuum. Aluminum attenuators were added to reduce the average alpha particle energy and range.

voltage values are compared to the known range values of the alpha particles after attenuation, it is found that the detector active width does not increase according to equation 10. In fact, the width dependence shows a V^K dependence where K is greater than one.

The detectors were exposed to 16 MeV X-rays from an electron accelerator in order to observe the pulse decay time and charge collection properties. The high energy of the X-rays ensures that ionization is evenly distributed throughout the detector volume. As the active region width extends across the detector with increasing bias voltage, the charge created in the active region is linearly proportional to its width. Therefore, by measuring the charge extracted from the active region, a relative measurement of the active region width as a function of bias voltage can be found. Figure 6 shows the results from a 760 micron detector in which the charge collected indicated a $V^{1.2}$ dependence on bias voltage. Thinner detectors (250 microns) showed a stronger dependence approaching $V^{1.6}$. The X-ray results support the alpha particle results in which we find that the active region width does not follow the $\sqrt{V}$ dependence. If trapping is considered, the measured charge is less than the actual charge created in the active region, suggesting that the dependence observed (value of K) is less than the real case. Carrier trapping may explain the decreasing value of K with increasing detector thickness.

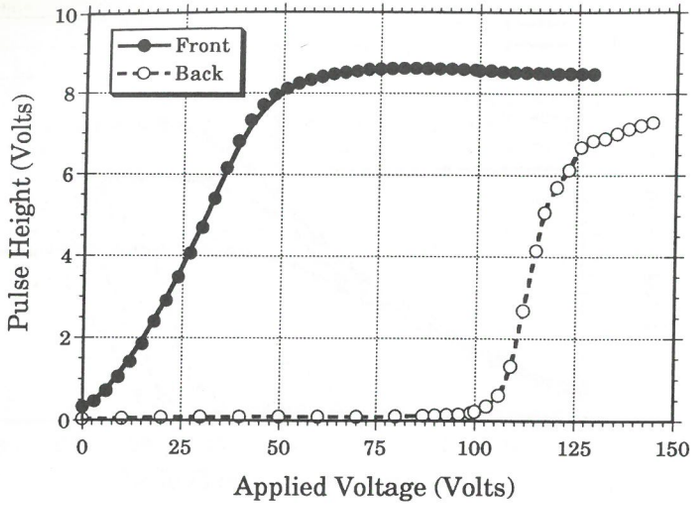

Figure 5. Measured voltage dependent pulse height response from a 105 micron GaAs Schottky diode detector. Shown are curves corresponding to front and back irradiation of the detector with 5.5 MeV ^{241}Am alpha particles in a vacuum.

It is believed that the deep level donors in the material are severely affecting the electric field distribution in the detectors. Semi-insulating LEC GaAs material is compensated by a balance of native defect deep donors EL2 (located 0.8 eV below the conduction band edge) with shallow carbon acceptor impurities[12]. Typically, carbon impurities are present in concentrations ranging from 10^{14} to 10^{15} per cm^3 and EL2 concentrations are reported to be on the order of 10^{16} per cm^3. The carbon impurities can be assumed fully ionized, however, the deep donor EL2 energy is slightly below the Fermi level and they are not fully ionized. The concentration of ionized EL2 sites can be described by the Fermi-Dirac distribution in which

$$N_d^+ = N_d\left[1 - \frac{1}{1 + \frac{1}{2}\exp(\frac{E_d - E_F}{kT})}\right] \tag{13}$$

where E_d is the deep donor energy and E_F is the Fermi energy. Substituting equation 13 into equation 9, the electric field distribution and net ionization concentration can be found numerically. With the boundary conditions $N_d = 10^{16}$, $N_a^- = 10^{14}$, and $V_B = 0.8$ volts, it is found that the EL2 deep donors become fully ionized at the Schottky contact and severely affect the electric field. Since the exact values of N_d and N_a are not known, the model serves to show an expected trend with the presence of a partially ionized deep donor rather than the exact values of the electric field distribution. The calculated electric field has two distinctively different regions[5]. Near the Schottky contact, the electric field decreases rapidly to low values.

Further into the detector bulk, the electric field decreases towards the ohmic contact more gradually. At any one value of electric field strength, the field is observed to move across the detector width as a function of V^K with K greater than one. The model suggests that the experimentally observed odd depletion characteristics are a consequence of the deep donors that compensate the material.

Pulse height measurements performed at room temperature resulted in observed full energy peaks from 5.5 MeV alpha particles. Resolution ranged from 2.2% to 3.1% FWHM with a typical resolution of 2.5% FWHM. The resolution improved with increasing bias voltage until the detector plateau voltages were reached ($\approx$ 55 volts). The resolution remained constant with increasing bias voltage beyond the plateau voltage. No degradation in detector resolution has been observed in a period of over one year of use. Assuming that the ionization energy for GaAs is 4.2 eV/e-h pair and the ionization energy for Si is 3.65 eV/e-h pair, the charge collection efficiency for Schottky contact irradiation of alpha particles as compared to a silicon surface barrier detector was 91% for a 43 micron detector and 82% for a 105 micron detector.

Room temperature measurements of gamma rays resulted in full energy peaks at 60 keV and 122 keV from ^{241}Am and ^{57}Co, respectively. The resolution was observed to be 22 keV (37%) at FWHM for 60 keV gamma rays and 40 keV (33%) at FWHM for 122 keV gamma rays. The poor resolution of gamma rays is believed to be a consequence of position dependent charge collection as described by equation 7. Measurements of gamma rays of energies higher than 122 keV resulted in a continuum with no observable full energy peak.

5. Conclusion

Detectors fabricated from semi-insulating undoped LEC GaAs were operated as alpha particle and gamma ray spectrometers at room temperature. The GaAs detectors were observed to have active region widths that deviated from $\sqrt{V}$ dependence expected from an abrupt junction analysis. Pulse height analysis with alpha particles and high energy X-rays indicated an active region width dependence of V^K with K greater than one. It was observed that the value of K decreased with increasing detector thickness which may be a consequence of carrier trapping. Numerical analysis indicates that full ionization of deep level donors can create a strong degradation in the electric field distribution through the detectors. It is hypothesized that the electric field degradation from deep donors is the mechanism by which the observed active region width deviates from $\sqrt{V}$ behavior and requires high voltages to extend across the detectors. The obvious next step is to fabricate detectors from material with a cumulative lower concentration of deep donors (or acceptors) and shallow dopant impurities in order to test the proposed hypothesis. In addition, new devices will be fabricated as *p-i-n* structures in order to improve the diode barrier heights, reduce leakage current, and reduce ohmic contact resistance.

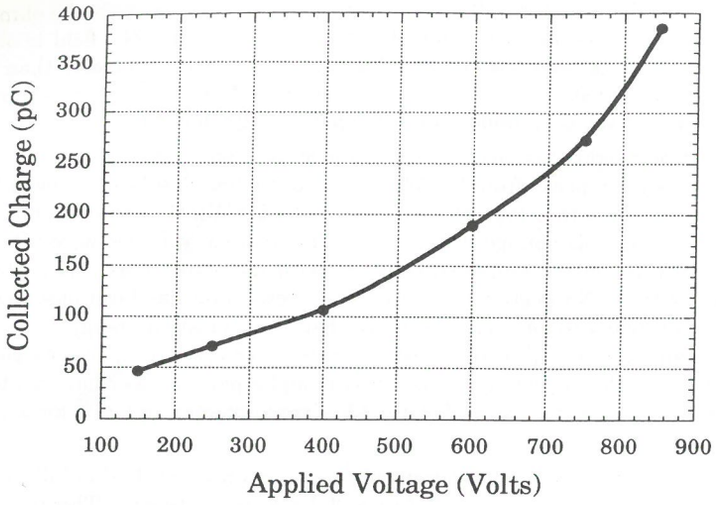

Figure 6. Total charge collected as a function of bias voltage for a 760 micron GaAs Schottky diode detector irradiated with 16 MeV X-rays.

6. Acknowledgements

We express our gratitude to David Brown, Alan Gibbs, and David Waechter of Los Alamos National Laboratory, William N. Gibler and Victor P. Swenson of Texas A&M University, and Jeff Fournier, Jim Kulman, Jim McCartney, and Ronald Rojeski of the University of Michigan for their technical assistance in the fabrication and analysis of the aforementioned GaAs detectors. We also express our gratitude to EG&G/EM in Santa Barbara for providing access to the US DOE linear accelerator. Proton implantation was performed by the Michigan Ion Beam Laboratory and detector fabrication was performed at the Solid State Electronics Laboratory, both located at the University of Michigan.

We express gratitude towards our colleagues Dr. Jack East and Dr. Fred L. Terry, Jr. at the University of Michigan for their valued collaboration with this project.

This project has been funded in part by Los Alamos National Laboratory subcontract 9-XGO-K7910-1.

7. References

1. G. Dearnaley and D.C. Northrop, *Semiconductor Detectors for Nuclear Radiations* (E.&F.N. Spon Ltd., London, 1963).
2. E. Sakai, *Nucl. Instr. and Meth.* 196 (1982) p. 121.
3. J.E. Eberhardt, R.D. Ryan, and A.J. Tavendale, *Nucl. Instr. and Meth.* 94 (1971) p. 463.
4. K. Hesse, W. Gramann, and D. Höppner, *Nucl. Instr. and Meth.* 101 (1972) p. 39.
5. D.S. McGregor, G.F. Knoll, Y. Eisen, and R. Brake, *IEEE Trans. Nucl. Sci., in press* (1992).
6. S.M. Sze, *Physics of Semiconductor Devices, 2nd. ed.* (J. Wiley & Sons, New York, 1981).
7. J.P. McKelvey, *Solid State and Semiconductor Physics* (Robert E. Kreiger Publishing Company, Malabar, 1966).
8. R.D. Evans, *The Atomic Nucleus* (Robert E. Kreiger Publishing Company, Malabar, 1955).
9. D. Look, *Electrical Characterization of GaAs Material and Devices* (J. Wiley & Sons, New York, 1989).
10. M. Shur, *GaAs Devices and Circuits* (Plenum Press, New York, 1987).
11. J.F. Ziegler and J.P. Biersack, *TRIM-90*, Version 90.05.
12. R.K. Willardson and A.C. Beer, *Semiconductors and Semimetals*, Vol. 20 (Academic Press, Inc., Orlando, 1984).